Int. J. Adv. Eng. Pure Sci. 2023, 35(2): 237-245
DOI: 10.7240/jeps.1240654

RESEARCH ARTICLE / ARAŞTIRMA MAKALESİ

Effect of Doping Concentration and Excitation Power on Upconversion and Temperature Sensitivity of $Gd_3Ga_5O_{12}:Yb^{3+}/Er^{3+}$ Phosphors

Hümeyra ÖRÜCÜ [1]

[1]*Ege University, Physics Department, 35040, Izmir, Turkey*

Abstract
Yb/Er codoped $Gd_3Ga_5O_{12}$ nanocrystalline upconverting phosphors were produced by the sol-gel pechini method at 1000 °C annealing temperature. The phosphor structure, morphological features, and luminescent properties of the fabricated material were studied using X-ray diffraction (XRD), transmission electron microscopy (TEM), high-resolution TEM (HR-TEM), and photoluminescence measurements (PL). Upconversion luminescence characteristics were investigated in the range of 450-850 nm by a 975 nm laser source. Emission, optical, and theoretical thermal behaviors were analyzed with respect to Er^{3+} ion content and the increasing excitation power. Temperature sensitivity calculations based on the fluorescence intensity ratio were performed by employing the thermally-coupled levels of Er^{3+}. The maximum sensitivity was calculated with the optimal value of $0.83x10^{-2}$ K^{-1} for $Gd_3Ga_5O_{12}$:2%Yb^{3+},0.5%Er^{3+} nanophosphor. The results pointed out that Yb/Er codoped $Gd_3Ga_5O_{12}$ may be a potential candidate for optical temperature sensors and lighting.
Keywords: Nanophosphors, upconversion, color parameters, optical temperature sensing, luminescence thermometers

I. INTRODUCTION

Trivalent rare earth ions doped inorganic host matrixes based on an upconversion process have been of great interest due to their convenient applications such as new generation of optical temperature sensors, lasers, display devices, solar cells in the visible region, and biomedical imaging [1–10]. Nowadays, the noncontact remote temperature measurement of phosphors based on the fluorescence intensity ratio (FIR) technique is applied on thermally coupled levels (TCLs) of rare earth ions for temperature sensitivity performance. The FIR technique is predicated on the concept of the Boltzmann distribution, which elucidates the manner in which electrons are allocated between two energy levels situated in close proximity. In the event that thermal energy causes the energy gap between these levels to be closed, a state of thermal equilibrium is attained, and the levels are designated as being thermally coupled. The method measures the ratio of the fluorescence intensities at two TCLs wavelengths, and the temperature of the material can be determined. The FIR method has advantages over other temperature measurement methods, including non-contact measurement, high sensitivity, and fast response time. The FIR method is commonly used in various industries, such as the high-magnetic field, biomedical research, and materials science, where precise temperature measurement is critical. The FIR technique has a higher sensitivity in a more comprehensive temperature range than other temperature measurement techniques [10–13].

Nanostructured Gd-based garnets are regarded as promising luminescence host materials due to having high chemical, physical, and thermal stability performance [14,15]. Gadolinium gallium garnet (GGG) has lower phonon energy (~650 cm^{-1}) and proven efficient host material that supports high concentrations of RE^{3+} substituted with Gd^{3+} ions without charge compensation [16,17].

Few research attempts have been focused on the temperature-sensing behavior of luminescence properties of gadolinium gallium garnet ($Gd_3Ga_5O_{12}$, GGG) [17–20]. Piao et al. studied ratiometric thermometry performance based on the FIR of the Er:$Gd_3Ga_5O_{12}$ single-crystal in the temperature range of 298–423 K and calculated (10.4–15.0) $\times10^{-3}$ K^{-1} relative sensitivities at 310 K [18]. Zhang et al. reported the low temperature sensitivity properties of $Gd_3Ga_5O_{12}:Yb^{3+}/Er^{3+}$ nanocrystals doped by Fe^{3+} in the temperature range from 300 K to 4.2 K [19]. Sun et al. demonstrated the optical thermometry properties of FIR of upconverted thermally coupled level emissions of Er:$Gd_3Ga_5O_{12}$ single crystal exhibiting (6.1–113.5)$\times10^{-3}$ K^{-1} relative sensitivity in the 100 K–430 K temperature range [20]. Kniec et al. measured the temperature-sensing performance of Cr^{3+}, Fe^{3+}, and Nd^{3+} codoped gadolinium gallium garnet nanocrystals [17].

Corresponding Author: Hümeyra ÖRÜCÜ, **Tel:** 0232 311 23 81, **e-posta:** humeyra.orucu@ege.edu.tr
Submitted: 22.01.2023, **Revised:** 20.03.2023, **Accepted:** 08.04.2023

In this sense, our research focused on optimizing upconversion luminescence properties of two-ion codoped gadolinium gallium garnet (GGG) nanophosphors. Our recent study reveals the energy transfer, and optical temperature sensitivity properties of Yb/Er co-doped GGG nano phosphors annealed at 800 °C and 1200 °C [16]. The position of peaks, emission intensity, emission band shape, and particle sizes of the nanophosphors are sensitively altered by the annealing temperature, doping concentration, and excitation power. In this study, the influence of Er^{3+} concentration and excitation power on upconversion luminescence, color, and laser-heat induced optical temperature performance of $Gd_3Ga_5O_{12}:Yb^{3+}/Er^{3+}$ nanophosphors annealed at 1000 °C are investigated in the range of 450-850 nm at room temperature.

II. MATERIALS AND METHODS

$Gd_3Ga_5O_{12}$ (Gadolinium Gallium Garnet) nanopowders doped with 2mol $\%Yb^{3+}$ and x mol $\%Er^{3+}$ (x=0.5, 1.0, 1.5, and 2.0) ions were prepared by the sol-gel pechini process and labeled as GGG:YE1, GGG:YE2, GGG:YE3, and GGG:YE4, respectively. $Gd(NO_3)_3{\cdot}6H_2O$, $Ga(NO_3)_3{\cdot}H_2O$, $Er(NO_3)_3{\cdot}5H_2O$ and $Yb(NO_3)_3{\cdot}5H_2O$ were used as the starting materials. All 99.99% pure salt products are purchased from Sigma-Aldrich. These raw chemicals were weighted out stoichiometric quantities based on the phase diagram of G_2O_3-Ga_2O_3 [21] and dissolved into the mixing aqueous HNO_3 solution. Citric acid and polyethylene glycol (PEG, average molecular weight: 3.350 $gmol^{-1}$) were mixed under continuous stirring at 65 ºC for three hours as a chelate ligand and a cross-linking agent, respectively. The mass of polyethylene glycol (PEG) was taken three times larger than the mass of citric acid. The obtained transparent sols aged for ten days at room temperature. Then prepared sols were annealed in a furnace at 1000 ºC, at a 7 C/min^{-1} for two hours. The optimized synthesis procedures and structural properties of nanophosphors by the sol-gel pechini method are reported in detail in a separate paper [16,22].

The upconversion luminescence spectra of the phosphors were recorded via Acton series-SI440 silicon detector attached to an SP2500i monochromator from Princeton Instruments. The samples were excited by A CNI MDL-H-975 model 975 nm continuous-wave laser diode. The laser pump power applied on the powders was determined through a Coherent Field MaxII-TOP Model power meter.

The morphological features and phase purity of the nanophosphors are determined by an X-ray diffractometer (Bruker AXS D8) in the range of 10° to 70° (2θ degree) and a high-resolution transmission electron microscope (HR-TEM) (FEI Inc. Tecnai G^2 20 Model).

III. RESULTS AND DISCUSSIONS

3.1. Structural Characterization

$Gd_3Ga_5O_{12}$ (GGG) garnet, which exists in cubic form with the Ia3d space group, is considered to be a promising host material for rare earth and transition metal ions. The XRD diagram of $Gd_3Ga_5O_{12}$ samples doped with a series of Yb^{3+}/Er^{3+} ions is demonstrated in Figure 1a. The Figure shows that most of the peaks well match the standard pattern of the cubic $Gd_3Ga_5O_{12}$ (Garnet) phase (PDF 13-0493). But there is also a small amount of a second weak orthorhombic Gd_3GaO_6 (Gallate) phase (PDF 53-1225). The content ratio of the dominant garnet phase is calculated as approximately 97% from the area under the most intense peaks in XRD spectra.

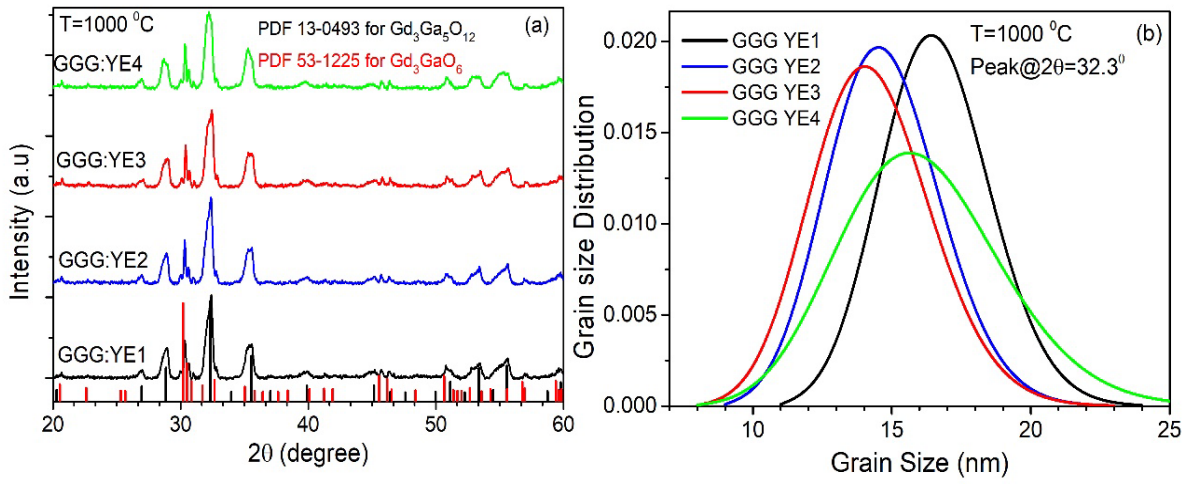

Figure 1. a) XRD patterns and **b)** Grain Size Distribution of GGG:Yb/Er nanophosphors annealed at 1000 °C

The grain size distribution (GSD) curves of the samples are illustrated using a powder diffraction line profile via $FW\frac{1}{5}/\frac{4}{5}$ method (Figure 1b), which is thought of as an expansion of the Scherrer method [21]. This method accepts that the grain sizes obey the Gamma distribution and takes into account full width at the 1/5 and 4/5 intensities of the most intense peak (θ=32.3°). The method with details can be found in reference [23]. The average sizes of nanocrystalline phosphors are in the range of 10 to 25 nm for 1000 °C annealing temperature. The GSD of the phosphors does not significantly change with increasing Er^{3+} concentration.

Figure 2 shows the TEM and HR-TEM images of GGG:2mol%Yb^{3+},1mol%Er^{3+} nanophosphors annealed at 1000 °C. Figure 2a illustrates the almost spherical shapes of the particles. The average crystal sizes obtained from TEM images are consistent with the sizes derived from the XRD pattern (The inset of Figure 2a). The high-resolution image reveals the inter-planar spacing and randomly oriented lattice fringes of the nanoparticles (NPs). Nanoparticles are highly crystallized as proven by well-resolved crystalline lattices. Partial overlapping of the lattice fringes in the HR-TEM image also indicates two phases within the nanoparticle.

3.2. Upconversion Characteristics

Among the rare earth ions, Yb and Er are the most efficient upconversion activators. Yb^{3+} ions have high absorption cross-section transition around 975 nm and can sensitize Er^{3+} ions by transferring the excitation energy [24,25]. For this reason, Er^{3+}-Yb^{3+} codoped materials have been widely researched as promising candidates for Luminescence thermometry recently [26–32].

The upconversion emission intensities of GGG:Yb/Er samples are recorded as a function of concentration between 450-850 nm wavelengths under 975 nm laser irradiation. As seen in Figure 3a and 3b, there are two distinct emission bands at the green and red regions for all samples measured at 4.1 and 22.4 W/cm^2 laser pump power, respectively. The spectral output of the samples represents that the upconversion emission intensities rise with increasing Er^{3+} content from 0.5% to 1%. In contrast, the intensities reduce with the further increasing 1mol% amount of Er^{3+} ions due to the concentration quenching. Figure 3c shows the integrated area of green and red regions as a function of % Er^{3+} concentration. The optimal Er^{3+} concentration is for $Gd_3Ga_5O_{12}$:2%Yb,1%Er. In the emission spectra, peaks are centered around 522.3, 527.4, 533.3, 537.6, 548.7, 555.1, and 559.2 nm at the green region and 653.5, 660.9, and 669.6 nm at the red region. The intensity of the red emissions is greater than the intensity of the green emissions. The relatively weak luminescence peaks around 490 nm at the blue region and 800 nm at the NIR region appear with the increasing laser pump power (Figure 3b). The moderate green, intense red, and weak NIR emission peaks correspond to the $^2H_{11/2}$, $^4S_{3/2} \rightarrow {}^4I_{15/2}$, $^4F_{9/2} \rightarrow {}^4I_{15/2}$, and $^4I_{9/2} \rightarrow {}^4I_{15/2}$ transitions of Er^{3+} at visible and NIR region, respectively (Figure 3b). Because of the cross-relaxations between Er^{3+} ions, NIR emission appears with the increasing pump power [16]. Blue emission, which is appeared between 480 and 500 nm, corresponds to the cooperative luminescence (CL) of Yb-Yb ion pairs (Figure 3b) [16].

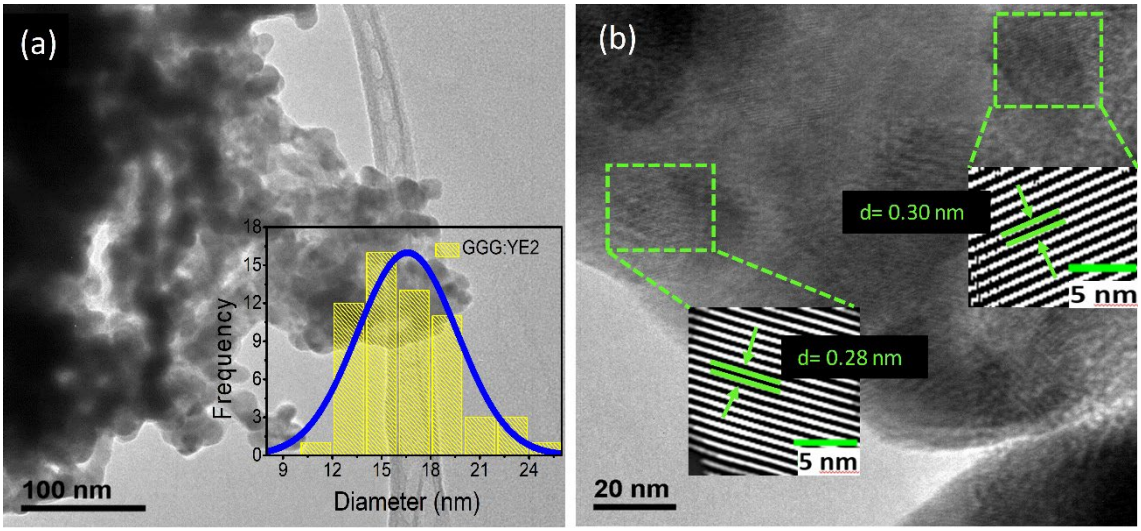

Figure 2. a) TEM, inset is the particle distribution histogram, and **b)** HR-TEM of GGG:2mol%Yb^{3+},1mol%Er^{3+} nanophosphors annealed at 1000 °C

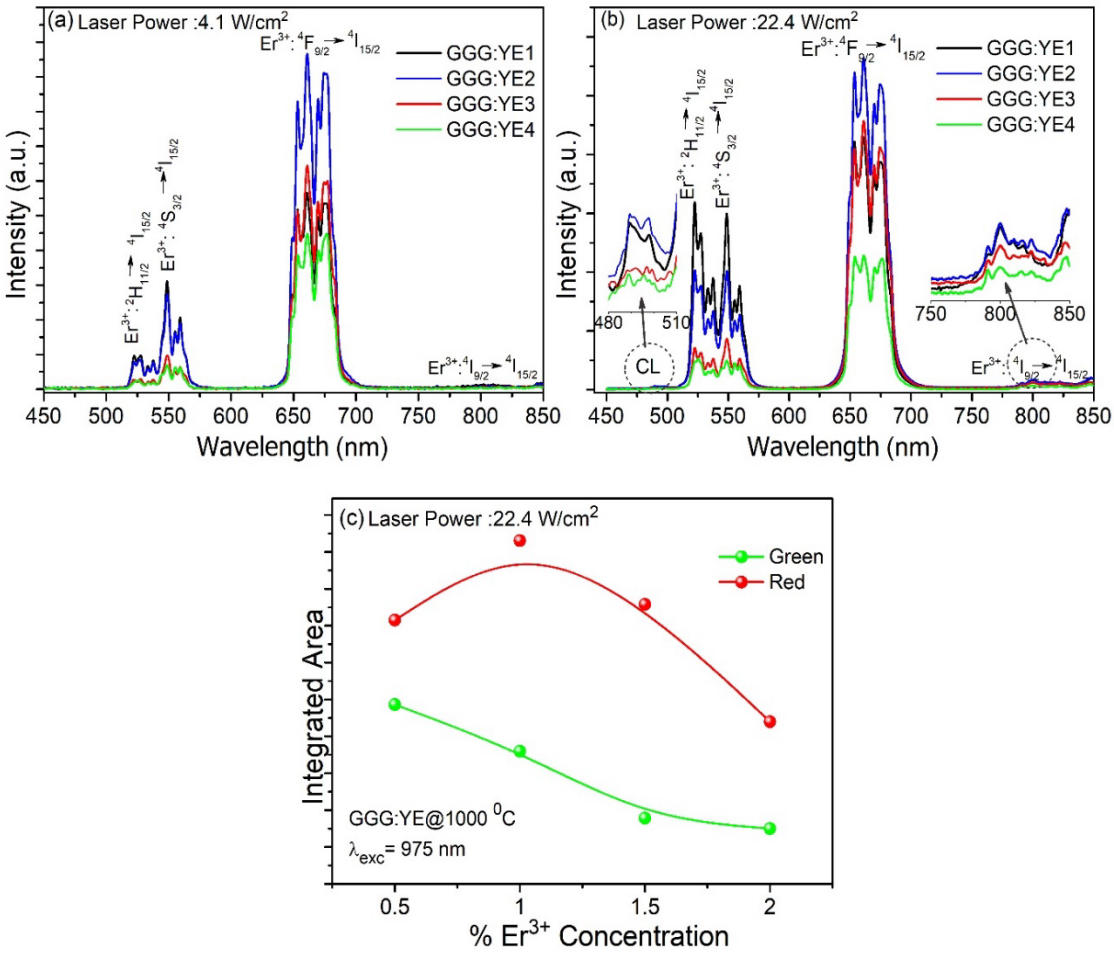

Figure 3. Upconversion emission intensities of the samples measured at **a)** 4.1 and **b)** 22.4 W/cm^2 **c)** the integrated area of green and red regions as a function of % Er^{3+} concentration

Power-dependent upconversion measurement was executed as the function of the laser pump power from 2.4 to 22.4 W/cm^2 under the laser excitation of 975 nm to clarify the upconversion mechanism. Figure 4a displays the upconversion emission spectra for $Gd_3Ga_5O_{12}$:2%Yb,1%Er nanophosphor as a function of pump power. The upconversion profiles remain the same, but emission intensities rise with rising pump power excitation due to the increase of excited Ytterbium ions that transfer energy to Erbium ions. Usually, luminescent intensity, I, and excitation pump power, P, obey the relation of $I \alpha P^n$ the power law. The number of photons (n) absorbed by activator and sensitizer ions to populate the excited state can be evaluated from the slope of logarithmic luminescent intensity versus logarithmic pump power graph. The plots of log(I) versus log(P) for 522.7 and 660.9 nm emissions of $Gd_3Ga_5O_{12}$:2%Yb,1%Er nanophosphor are demonstrated in Figure 4b. The n values of green and red emissions were $n_{522.7}$ = ~1.8 and $n_{660.9}$= ~1.4, respectively. The sufficient energy transfer from Ytterbium to Erbium and possible saturation processes can be in charge of the reduced n values [33]. The green and red region emissions of Er^{3+} ions participate in the two-photon absorption process.

3.3. Temperature Sensing Characteristics

Luminescence temperature sensing is a potential candidate for a noncontact remote measurement option in several situations that traditional thermometer is not able to perform, such as in the electromagnetic field, a circuit with a small size below 10 μm, a high-voltage power station, a coal mine, a micro-fluid, and a moving object [10,34,35].

The influence of temperature on the luminescence intensity is determined by the fluorescence intensity ratio (FIR), which is based on the Boltzmann distribution of electrons between the two thermally coupled energy levels (TCLs). These two thermally coupled levels (TCLs) of Er^{3+}:$^2H_{11/2}$ and Er^{3+}:$^4S_{3/2}$ to $^4I_{15/2}$ ground state were selected as 522.7 nm and 548.7 nm for fluorescence intensity ratio (FIR) thermometry.

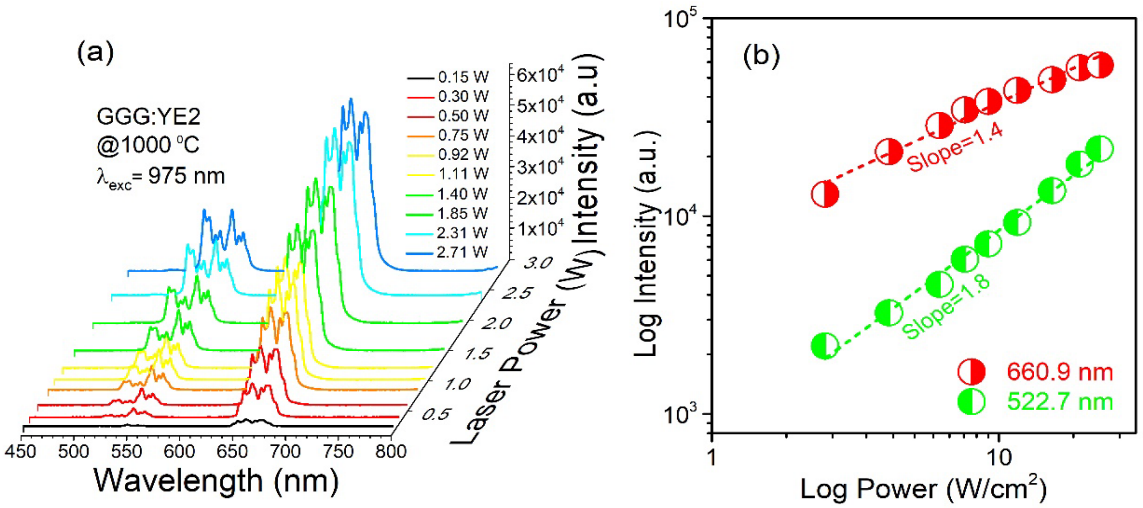

Figure 4. a) Room temperature upconversion luminescence spectra of GGG:YE2 **b)** The log-log plots of upconversion luminescence intensity as a function of power for GGG:YE2

The change in energy (ΔE) between these levels is calculated as 906.54 cm^{-1}. The dependences of FIR-TCL ($I_{522.7}/I_{548.7}$), values on the pump power were analyzed in Figure 5a. The FIR-TCL values displayed an upward trend with the elevated laser pump power. The data fitted linearly. The inset of Figure 5a shows the upconversion emissions of GGG:2%Yb, 0.5%Er nanophosphor at different pump powers. The relationship between the thermally coupled levels (TCLs) and temperature is defined by the Boltzmann distribution law [12,13]:

$$FIR = \frac{I_{522.7}}{I_{548.7}} = Bexp\left(\frac{-\Delta E}{kT}\right) \quad \textbf{(1)}$$

where $I_{522.7}$ and $I_{548.7}$ are the integrated intensities of thermally coupled levels, B is the constant, ΔE is the energy difference between the thermally coupled levels, k is Boltzman's coefficient, and T is the absolute temperature.

When the laser pump power elevates, the temperature of the samples increases regardless of the environment temperature. Evidently, The FIR values also represented a linear upward trend with the elevated pump power (Figure 5a). According to the FIR equation, a certain FIR value corresponds to a phosphor sample temperature. The precise value of the temperature can be derived from the FIR equation. For example, if the spectral energy difference was used in equation (1) at room temperature and at the lowest pump power, the coefficient of B is calculated as 24.5 for 2%Yb^{3+}/1%Er^{3+}: $Gd_3Ga_5O_{12}$ phosphor. Afterward, the equation below can be utilized to define the phosphor temperature for a particular pump power:

$$T = \left(\frac{1}{lnB - \ln(FIR)}\right) x \frac{\Delta E}{k} \quad \textbf{(2)}$$

Using equation (2), the phosphor temperatures at various pump powers were calculated, and corresponding values are shown in Figure 5b for nanophosphors. The phosphor temperatures for all samples vary linearly from 300 K to 420 K with rising pump power from 0.5 W to 3 W. Both GGG:YE1-YE2 and GGG:YE3-YE4 show similar behavior. It is depicted that phosphor temperature can be adjusted by changing the dopant concentrations as a function of pump power.

Moreover, absolute (S_A) and relative sensor sensitivities (S_R) are two critical thermometric evaluation criteria. They can be depicted by the following equations [12,13]:

$$S_A = \frac{d(FIR)}{dT} = Bexp\left(\frac{-\Delta E}{kT}\right) x \frac{\Delta E}{kT^2} \quad \textbf{(3)}$$

$$S_R = \left|\frac{1}{FIR}\frac{d(FIR)}{dT}\right| \quad \textbf{(4)}$$

The calculated phosphor temperature corresponding to pump powers versus temperature-dependent sensitivities is presented in Figure 5c. The S_A value rose with the increase of temperature and found its maximum value of 0.0083 K^{-1} at 414 K, whereas the maximum value of S_R was about 14.7x$10^{-3}K^{-1}$ at 300 K for 2%Yb^{3+},0.5%Er^{3+}:GGG. The absolute sensitivity values reduce with the rising Er^{3+} dopant content. The S_A values are calculated as 0.0077 K^{-1} at 416 K, 0.0071 K^{-1} at 391 K, and 0.0070 K^{-1} at 390 K for GGG:YE2, GGG:YE3, and GGG:YE4, respectively. The temperature value at which the highest sensitivity was reached for the current study increased in contrast to other materials examined with rare earth elements doped GGG in the literature [17–20].

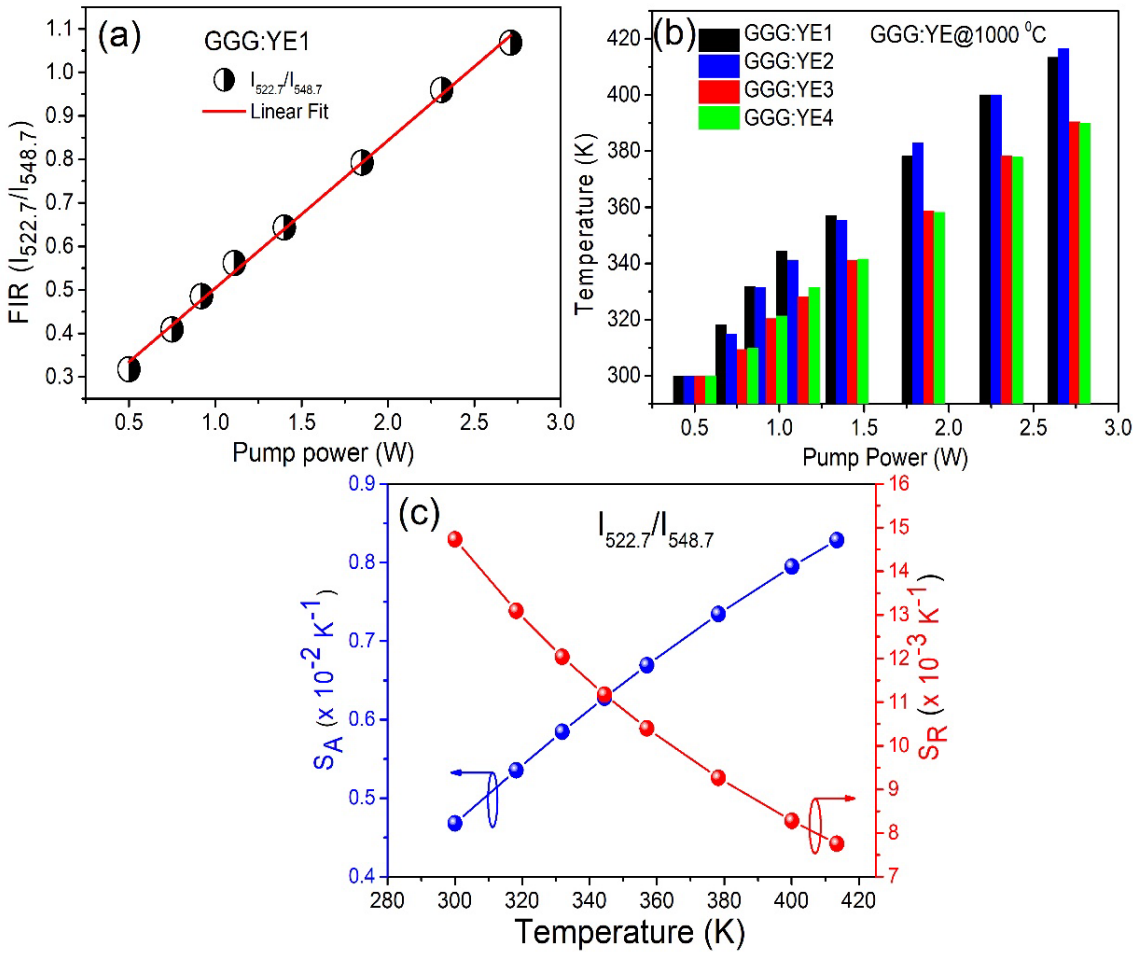

Figure 5. a) FIR values of thermally coupled levels (TCLs) versus pump power **b)** Calculated Phosphor temperature versus pump power **c)** Sensitivities based on TCLs versus temperature

3.4. Color Characteristics

The chromaticity (CIE) coordinates were calculated from the spectra utilizing the 1931 CIE system. Figure 6 demonstrates the corresponding CIE diagram of $Gd_3Ga_5O_{12}$:2%Yb^{3+}/x%Er^{3+} phosphors (0.5≤ x ≤2.0) with distinct Er^{3+} doping concentrations. The color coordinates of the nanophosphors shift from yellowish to the greenish area with increasing pump power (Figure 6a and 6b). When Er^{3+} doping concentration changed from 0.5 to 2.0 mol%, the chromaticity coordinates (x, y) changed significantly from yellowish green to yellowish orange at the pumping power of 22.4 W/cm^2 (Figure 6c).

The exact values of the chromaticity coordinates (x, y) are (0.333, 0.333) for the white zone. CIE coordinates of the nanophosphors are summarized in Table 1. The result denotes that as GGG:Yb/Er samples show multicolor luminescence in the visible region when excited by monochromatic light, they might find potential application in the display systems.

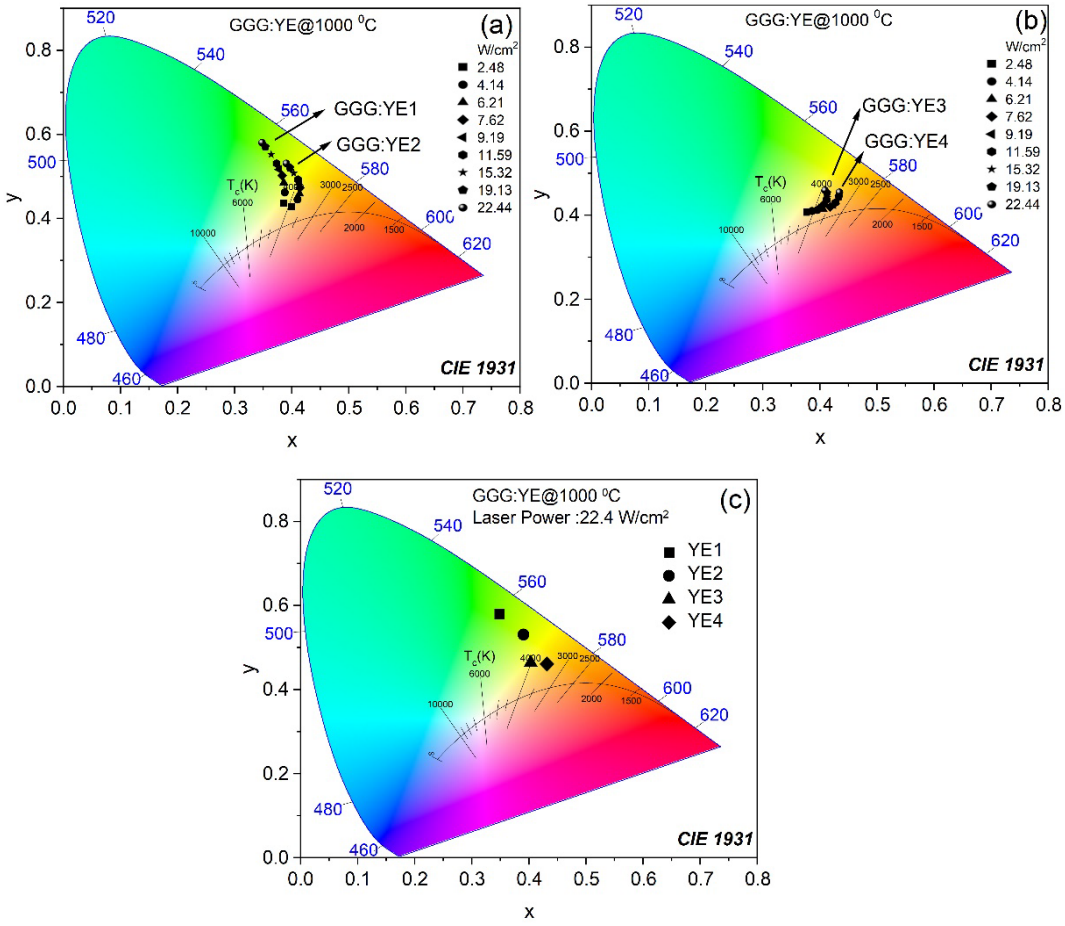

Figure 6. The color coordinates of the phosphors in the CIE diagram

Table 1. CIE color coordinates of the nanophosphors

Power (W)	YE1		YE2		YE3		YE4	
	x	y	x	y	x	y	x	y
0.15	0.376	0.413	0.379	0.411	0.376	0.409	0.376	0.408
0.30	0.385	0.437	0.399	0.428	0.386	0.410	0.395	0.412
0.50	0.388	0.462	0.410	0.445	0.399	0.416	0.406	0.415
0.75	0.386	0.485	0.414	0.459	0.405	0.423	0.418	0.420
0.92	0.383	0.502	0.415	0.473	0.410	0.429	0.424	0.425
1.11	0.378	0.516	0.414	0.481	0.412	0.437	0.427	0.430
1.40	0.374	0.531	0.411	0.492	0.413	0.442	0.431	0.434
1.85	0.364	0.552	0.404	0.507	0.412	0.453	0.433	0.444
2.31	0.354	0.570	0.397	0.521	0.409	0.459	0.434	0.454
2.71	0.348	0.580	0.391	0.531	0.403	0.465	0.432	0.460

IV. CONCLUSION

The luminescence intensity of the phosphors strongly depends on the conditions of their preparation methods, the choice of the host materials and doped ions, the concentration of the doped ions, and the particle size of the samples. In this study, the upconversion, color, and laser-heat induced optical temperature sensing behavior of $Gd_3Ga_5O_{12}$:Yb^{3+}/Er^{3+} phosphors synthesized by the sol-gel pechini method at 1000 °C are reported. The wavelength range for the upconversion emission spectrum is between 450-850 nm. The influence of Er^{3+} and Yb^{3+} ion concentrations on the intensity of upconversion luminescence was also studied in detail under the 975 nm excitation wavelength. The Er^{3+}/Yb^{3+} codoped gadolinium gallium garnet nanophosphor gives green emission bands at 522.7 and 548.7 nm upon 975 nm excitation due to $^2H_{11/2}$ and $^4S_{3/2}$ to $^4I_{15/2}$ transitions of Er^{3+} ion, respectively. The fluorescence intensity ratio (FIR) of the 522.7 and 548.7 nm emission bands of the phosphors vary with the increase in concentration and laser pump power. The FIR of the thermally coupled 522.7 and 548.7 nm emission bands displays significant optical heating in the codoped phosphor. It is indicated that phosphor temperature can be adjusted by changing the dopant concentrations as a function of pump power. The maximum absolute temperature sensitivity has been calculated to be 0.0083 K^{-1} at 414 K, whereas the maximum value of relative sensitivity was about $14.7x10^{-3}K^{-1}$ at 300 K for 2%Yb^{3+},0.5%Er^{3+}:GGG. The present study on Er^{3+}/Yb^{3+} codoped gadolinium gallium garnet (GGG) nanophosphors achieved a higher maximum sensitivity temperature compared to other rare earth element-doped GGG materials studied in the literature. Additionally, the study suggests that the dopant concentration for this particular nanophosphor has been optimized. Color coordinates on the CIE diagram of phosphors were influenced by the pump power and shifted from yellowish green to yellowish orange region at higher Er^{3+} concentrations. Thus, the Er^{3+}/Yb^{3+} codoped gadolinium gallium garnet nano-phosphor can be useful for photonic devices such as an optical heater, nano phosphor temperature sensors, and solid-state lighting.

REFERENCES

[1] Daldosso, M., Falcomer, D., Speghini, A., Bettinelli, M., Enzo, S., Lasio, B., & Polizzi, S. (2008). Synthesis, structural investigation and luminescence spectroscopy of nanocrystalline $Gd_3Ga_5O_{12}$ doped with lanthanide ions. *J. Alloys Compd.,* 451(1–2), 553–556.

[2] Venkatramu, V., León-Luis, S. F., Rodríguez-Mendoza, U. R., Monteseguro, V., Manjón, F. J., Lozano-Gorrín, A. D., Valiente, R., Navarro-Urrios, D., Jayasankar, C. K., Muñoz, A., & Lavín, V. (2012). Synthesis, structure and luminescence of Er $^{3+}$-doped $Y_3Ga_5O_{12}$ nano-garnets. *J. Mater. Chem.,* 22(27), 13788–13799.

[3] Singh, S. K., Lee, D. G., Yi, S. S., Jang, K., Shin, D. S., & Jeong, J. H. (2013). Probing dual mode emission of Eu^{3+} in garnet phosphor. *J. Appl. Phys.,* 113(17).

[4] Wang, X., Li, X., Xu, S., Cheng, L., Sun, J., Zhang, J., Li, L., & Chen, B. (2019). A comparative study of spectral and temperature sensing properties of Er^{3+} mono-doped $LnNbO_4$ (Ln = Lu, Y, Gd) phosphors under 980 and 1500 nm excitations. *Mater. Res. Bull.,* 111, 177–182.

[5] Ranjan, S. K., Mondal, M., & Rai, V. K. (2018). Er^{3+}-Yb^{3+}/Er^{3+}-Yb^{3+}-Li^{+}/Er^{3+}-Yb^{3+}-Zn^{2+}:Gd_2O_3 nanophosphors for efficient frequency upconverter and temperature sensing applications. *Mater. Res. Bull.,* 106, 66–73.

[6] Liu, X., Lei, R., Huang, F., Deng, D., Wang, H., Zhao, S., & Xu, S. (2019). Dependence of upconversion emission and optical temperature sensing behavior on excitation power in Er^{3+}/Yb^{3+} co-doped $BaMoO_4$ phosphors. *J. Lumin.,* 210, 119–127.

[7] Du, P., Luo, L., & Yu, J. S. (2015). Infrared-to-visible upconversion emission of Er^{3+}/Yb^{3+}-codoped SrMoO4 phosphors as wide-range temperature sensor. *Curr. Appl. Phys*, 15(12), 1576–1579.

[8] Lu, H., Hao, H., Gao, Y., Shi, G., Fan, Q., Song, Y., Wang, Y., & Zhang, X. (2017). Dual functions of Er^{3+}/Yb^{3+} codoped $Gd_2(MoO_4)_3$ phosphor: temperature sensor and optical heater. *J. Lumin.,* 191, 13–17.

[9] Ćirić, A., Stojadinović, S., & Dramićanin, M. D. (2020). Luminescence temperature sensing using thin-films of undoped Gd_2O_3 and doped with Ho^{3+}, Eu^{3+} and Er^{3+} prepared by plasma electrolytic oxidation. *Ceram. Int.*, 46(14), 23223–23231.

[10] Vetrone, F., Naccache, R., Zamarrón, A., De La Fuente, A. J., Sanz-Rodríguez, F., Maestro, L. M., Rodriguez, E. M., Jaque, D., Sole, J. G., & Capobianco, J. A. (2010). Temperature sensing using fluorescent nanothermometers. *ACS Nano.*, 4(6), 3254–3258.

[11] Marciniak, L., & Trejgis, K. (2018). Luminescence lifetime thermometry with Mn^{3+}-Mn^{4+} co-doped nanocrystals. *J. Mater. Chem. C.,* 6(26), 7092–7100.

[12] Wade, S.A., Collins, S.F., Baxter, G.W. (2003) Fluorescence intensity ratio technique for optical fiber point temperature sensing, J. *Appl. Phys,.* 94, 4743–4756.

[13] Wang, X., Liu, Q., Bu, Y., Liu, C.S., Liu, T., Yan, X. (2015) Optical temperature sensing of rare-earth ion doped phosphors, *RSC Adv.*, 5, 86219–86236.

[14] Pang, M., & Lin, J. (2005). Growth and optical properties of nanocrystalline $Gd_3Ga_5O_{12}$: Ln (Ln = Eu^{3+}, Tb^{3+}, Er $^{3+}$) powders and thin films via Pechini sol-gel process. *J. Cryst. Growth.,* 284(1–2), 262–269.

[15] Li, Y., Lu, H., Zhang, Y., Ma, J., & Song, G. (2012). Synthesis and luminescence properties of nanocrystalline $Gd_3Ga_5O_{12}:Eu^{3+}$ by a homogeneous precipitation method. *Rare Met.,* 31(6), 599–603.

[16] Erdem, M., Örücü, H., Cantürk, S. B., & Eryürek, G. (2021). Upconversion Yb^{3+}/Er^{3+}:Gadolinium Gallium Garnet Nanocrystals for White-Light Emission and Optical Thermometry. *ACS Appl. Nano Mater.,* 4(7), 7162–7171.

[17] Kniec, K., Ledwa, K., MacIejewska, K., & Marciniak, L. (2020). Intentional modification of the optical spectral response and relative sensitivity of luminescent thermometers based on Fe^{3+},Cr^{3+},Nd^{3+}co-doped garnet nanocrystals by crystal field strength optimization. *Mater. Chem. Front.,* 4(6), 1697–1705.

[18] Piao, R. Q., Xu, Q., Zhang, Z. B., Wang, Y., Pun, E. Y. B., & Zhang, D. L. (2018). A study on ratiometric thermometry based on upconversion emissions of erbium ions in gadolinium gallium garnet single-crystal. *J. Lumin.,* 204, 116–121.

[19] Zhang, K., Tong, L., Ma, Y., Wang, J., Xia, Z., & Han, Y. (2019). Modulated up-conversion luminescence and low-temperature sensing of $Gd_3Ga_5O_{12}:Yb^{3+}/Er^{3+}$ by incorporation of Fe^{3+} ions. *J. Alloys Compd.*, 781, 467–472.

[20] Sun, H. X., Yuan, N., Zhang, Z. B., Sun, Q., Wang, Y., Wong, W. H., Tu, C. Y., Yu, D. Y., Pun, E. Y. B., & Zhang, D. L. (2017). Temperature characteristics of the green up-conversion fluorescence of Er^{3+}-doped $Gd_3Ga_5O_{12}$ single crystal for temperature sensing. *Sci. Adv. Mater.,* 9(5), 727–732.

[21] Garino, T. J., Voigt, J. A., Spoerke, E. D., Moore, D. L., Lockwood, S. J., Gibson, J. T., & Phifer, C. C. (2007). Development of a Manufacturing Capability for Production of Ceramic Laser Materials. No. SAND2007-7393. Sandia National Laboratoires Report

[22] Örücü, H. (2022). The effect of molar ratio and annealing on crystal structure of gadolinium-gallium garnet nanopowders synthesized by sol-gel method. *J. Ceram. Process. Res.*, 23(6), 799–805.

[23] Pielaszek, R. (2004). FW 1/5/4/5 M method for determination of the grain size distribution from powder diffraction line profile. *J. Alloys Compd.*, 382(1–2), 128–132.

[24] Guo, Y., Wang, D., Zhao, X., & Wang, F. (2016). Fabrication, microstructure and upconversion luminescence of Yb^{3+}/Ln^{3+} (Ln = Ho, Er, Tm) co-doped $Y_2Ti_2O_7$ ceramics. *Mater. Res. Bull.,* 73, 84–89.

[25] Santana-Alonso, A., Méndez-Ramos, J., Yanes, A. C., Del-Castillo, J., & Rodríguez, V. D. (2010). White light up-conversion in transparent sol-gel derived glass-ceramics containing Yb^{3+}-Er^{3+}-Tm^{3+} triply-doped YF_3 nanocrystals. *Mater. Chem. Phys.,* 124(1), 699–703.

[26] Wang, X., Wang, Y., Jin, L., Bu, Y., Yang, X. L., & Yan, X. (2019). Controlling optical temperature detection of $Ca_3Al_2O_6$: Yb^{3+},Er^{3+} phosphors through doping. *J. Alloys Compd.*, 773, 393–400.

[27] Liao, J., Wang, Q., Kong, L., Ming, Z., Wang, Y., Li, Y., & Che, L. (2018). Effect of Yb^{3+} concentration on tunable upconversion luminescence and optically temperature sensing behavior in $Gd_2TiO_5:Yb^{3+}/Er^{3+}$phosphors. *Opt. Mater.*, 75, 841–849.

[28] Cheng, X., Dong, X., Peng, K., Zhang, H., Su, Y., & Jiang, L. (2020). Upconversion Luminescence and Optical Temperature-Sensing Properties of $LaNbO_4:Yb^{3+}/Er^{3+}$ Phosphors. *J. Electron. Mater.,* 49(1), 518–523.

[29] Lin, M., Xie, L., Wang, Z., Richards, B. S., Gao, G., & Zhong, J. (2019). Facile synthesis of mono-disperse sub-20 nm $NaY(WO_4)_2:Er^{3+}$,Yb^{3+} upconversion nanoparticles: A new choice for nanothermometry. *J. Mater. Chem. C.,* 7(10), 2971–2977.

[30] Gao, P., Li, X., Gong, Y., Shen, G., Zhang, S., & Guan, L. (2019). Highly sensitive up-conversion phosphor for optical thermometry: $CaLaAl_3O_7:Er^{3+}/Yb^{3+}$. *J. Rare Earths.,* 37(9), 937–942.

[31] Du, P., Luo, L., & Yu, J. S. (2016). Facile synthesis of Er^{3+}/Yb^{3+}-codoped $NaYF_4$ nanoparticles: A promising multifunctional upconverting luminescent material for versatile applications. *RSC Adv.*, 6(97), 94539–94546.

[32] Liu, H., Jian, X., Liu, M., Wang, K., Bai, G., & Zhang, Y. (2021). Investigation on the upconversion luminescence and ratiometric thermal sensing of $SrWO_4:Yb^{3+}/RE^{3+}$(RE = Ho/Er) phosphors. *RSC Adv.*, 11(58), 36689–36697.

[33] Pollnau, M., Gamelin, D., Lüthi, S., Güdel, H., & Hehlen, M. (2000). Power dependence of upconversion luminescence in lanthanide and transition-metal-ion systems. *Phys. Rev. B - Condens. Matter Mater. Phys.*, 61(5), 3337–3346.

[34] Liu, X., Chen, Y., Shang, F., Chen, G., & Xu, J. (2019). Wide-range thermometry and up-conversion luminescence of $Ca_5(PO_4)_3$ $F:Yb^{3+}$ /Er^{3+} transparent glass ceramics. *J. Mater. Sci. Mater. Electron.*, 30(6), 5718–5725.

[35] Fischer, L. H., Harms, G. S., & Wolfbeis, O. S. (2011). Upconverting nanoparticles for nanoscale thermometry. *Angew. Chemie - Int. Ed.,* 50(20), 4546–4551.